

Original Article

# Enhancing the potency of lithospermate B for inhibiting Na<sup>+</sup>/K<sup>+</sup>-ATPase activity by forming transition metal ion complexes

Nan-Hei LIN<sup>1, #</sup>, Tse-Yu CHUNG<sup>1, #</sup>, Feng-Yin LI<sup>2</sup>, Hsin-An CHEN<sup>3, 4, \*</sup>, Jason TC TZEN<sup>1, 5, 6, \*</sup>

<sup>1</sup>Graduate Institute of Biotechnology and <sup>2</sup>Department of Chemistry, National Chung Hsing University, Taichung 40227, Taiwan, China; <sup>3</sup>Division of General Surgery, Department of Surgery, Shuang Ho Hospital, Taipei Medical University, Taipei 11031, Taiwan, China; <sup>4</sup>Graduate Institute of Clinical Medicine, College of Medicine, Taipei Medical University, Taipei 11031, Taiwan, China; <sup>5</sup>School of Chinese Medicine, China Medical University, Taichung 40402, Taiwan, China; <sup>6</sup>Agricultural Biotechnology Research Center, Academia Sinica, Taipei 11529, Taiwan, China

**Aim:** To determine whether replacing Mg<sup>2+</sup> in magnesium lithospermate B (Mg-LSB) isolated from danshen (*Salvia miltiorrhiza*) with other metal ions could affect its potency in inhibition of Na<sup>+</sup>/K<sup>+</sup>-ATPase activity.

**Methods:** Eight metal ions (Na<sup>+</sup>, K<sup>+</sup>, Mg<sup>2+</sup>, Cr<sup>3+</sup>, Mn<sup>2+</sup>, Co<sup>2+</sup>, Ni<sup>2+</sup>, and Zn<sup>2+</sup>) were used to form complexes with LSB. The activity of Na<sup>+</sup>/K<sup>+</sup>-ATPase was determined by measuring the amount of inorganic phosphate (Pi) liberated from ATP. Human adrenergic neuroblastoma cell line SH-SY5Y was used to assess the intracellular Ca<sup>2+</sup> level fluctuation and cell viability. The metal binding site on LSB and the binding mode of the metal-LSB complexes were detected by NMR and visible spectroscopy, respectively.

**Results:** The potencies of LSB complexed with Cr<sup>3+</sup>, Mn<sup>2+</sup>, Co<sup>2+</sup>, or Ni<sup>2+</sup> increased by approximately 5 times compared to the naturally occurring LSB and Mg-LSB. The IC<sub>50</sub> values of Cr-LSB, Mn-LSB, Co-LSB, Ni-LSB, LSB, and Mg-LSB in inhibition of Na<sup>+</sup>/K<sup>+</sup>-ATPase activity were 23, 17, 26, 25, 101, and 128 μmol/L, respectively. After treatment of SH-SY5Y cells with the transition metal-LSB complexes (25 μmol/L), the intracellular Ca<sup>2+</sup> level was substantially elevated, and the cells were viable for one day. The transition metals, as exemplified by Co<sup>2+</sup>, appeared to be coordinated by two carboxylate groups and one carbonyl group of LSB. Titration of LSB against Co<sup>2+</sup> demonstrated that the Co-LSB complex was formed with a Co<sup>2+</sup>:LSB molar ratio of 1:2 or 1:1, when [Co<sup>2+</sup>] was less than half of the [LSB] or higher than the [LSB], respectively.

**Conclusion:** LSB complexed with Cr<sup>3+</sup>, Mn<sup>2+</sup>, Co<sup>2+</sup>, or Ni<sup>2+</sup> are stable, non-toxic and more potent in inhibition of Na<sup>+</sup>/K<sup>+</sup>-ATPase. The transition metal-LSB complexes have the potential to be superior substitutes for cardiac glycosides in the treatment of congestive heart failure.

**Keywords:** cardiac glycoside; lithospermate B; *Salvia miltiorrhiza*; transition metal; metal complex; Na<sup>+</sup>/K<sup>+</sup>-ATPase; congestive heart failure; traditional Chinese medicine

Acta Pharmacologica Sinica (2013) 34: 893–900; doi: 10.1038/aps.2013.32; published online 20 May 2013

## Introduction

Na<sup>+</sup>/K<sup>+</sup>-ATPase is responsible for the active transport of sodium and potassium ions, and it is essential for maintaining membrane potentials, cell volume, and the active transport of other solutes in animal cells<sup>[1]</sup>. In addition, this enzyme is a P-type ATPase, also known as a sodium pump, which commonly consumes 20%–30% of the adenosine triphosphate

(ATP) energy generated in animal cells at rest to actively transport three Na<sup>+</sup> out of the cell and two K<sup>+</sup> into the cell<sup>[2]</sup>. The Na<sup>+</sup>/K<sup>+</sup>-ATPase structure comprises three subunits, termed the α, β, and γ subunits, that execute distinct biological functions<sup>[3–5]</sup>. The sites for ATP binding, phosphorylation and ion occlusion are located in the α subunit. This subunit also contains an inhibitor-binding cavity that serves as the primary target for many pharmacological agents, such as cardiac glycosides<sup>[6–8]</sup>.

The therapeutic effect of cardiac glycosides in the treatment of congestive heart failure derives from their reversible inhibition of the Na<sup>+</sup>/K<sup>+</sup>-ATPase located in the cell membrane of the human myocardium<sup>[9, 10]</sup>. This inhibition leads to the

# These two authors contributed equally to this work.

\* To whom correspondence should be addressed.

E-mail dtsurga6@gmail.com (Hsin-An CHEN);

TCTZEN@dragon.nchu.edu.tw (Jason TC TZEN)

Received 2012-12-13 Accepted 2013-03-11

accumulation of sodium in cardiac cells, the promotion of the sodium-calcium exchange system in the cell membrane, and ultimately, a higher level of intracellular and myocardial calcium<sup>[11]</sup>. The elevated intracellular calcium concentration results in an increased inotropism, accentuating the force of myocardial contractions by increasing the velocity and extent of sarcomere shortening. In other words, there is increased stroke work for a given filling volume of pressure<sup>[12]</sup>. Although inhibition of the Na<sup>+</sup>/K<sup>+</sup>-ATPase produces beneficial effects in patients with congestive heart failure, cardiac glycosides have severe side effects and a narrow therapeutic index, limiting their clinical applications<sup>[13]</sup>.

Recently, a number of steroid-like compounds from diverse Chinese medicinal products used for promoting blood circulation were demonstrated to be effective inhibitors of Na<sup>+</sup>/K<sup>+</sup>-ATPase; thus, these compounds could exert therapeutic cardiac effects via the same molecular mechanisms as cardiac glycosides<sup>[14-18]</sup>. Exceptionally, no appreciable steroid-like compound content was found in danshen (*Salvia miltiorrhiza*), a well-known Chinese herb traditionally used for promoting blood circulation<sup>[19]</sup>. Instead, magnesium lithospermate B (Mg-LSB), the major soluble ingredient in danshen, was demonstrated to be a strong inhibitor of Na<sup>+</sup>/K<sup>+</sup>-ATPase and is regarded as the active ingredient responsible for the therapeutic cardiac effect of this herb<sup>[20]</sup>. Mg-LSB may have the potential to be a substitute for cardiac glycosides in the treatment of congestive heart failure because it is a non-toxic antioxidant and appears to have no adverse effects; however, clinical trials assessing the efficacy of this compound are lacking<sup>[21]</sup>.

Mg-LSB possesses a relatively rigid structure as a result of the formation of salt bridges between Mg<sup>2+</sup> and the four oxygen atoms of the carboxyl groups that originated from the four caffeic acid fragments<sup>[22]</sup>. The rigid structure around the salt bridges formed between Mg<sup>2+</sup> and the carboxyl groups partially mimics the core steroid structure of cardiac glycosides. To develop more effective drugs for the treatment of congestive heart failure, we sought to determine whether the magnesium ion of Mg-LSB could be replaced with other metal ions to form complexes with a higher potency for inhibiting Na<sup>+</sup>/K<sup>+</sup>-ATPase activity. In this study, abundant metal ions and trace transition metal ions found in the human body were used to form soluble complexes with LSB. The potency of these complexes for inhibiting Na<sup>+</sup>/K<sup>+</sup>-ATPase activity and their cytotoxicity was evaluated. As exemplified by the formation of a Co-LSB complex, the transition metal binding site in LSB and the binding modes with different ratios of Co<sup>2+</sup> to LSB were also examined.

## Materials and methods

### Chemicals and reagents

Purified LSB was obtained from KO DA Pharmaceutical Company (Taiwan, China). Mg(OH)<sub>2</sub> was purchased from Showa Chemical Co (Japan). NaOH, KOH, CrCl<sub>3</sub>, MnCl<sub>2</sub>, CoCl<sub>2</sub>, and NiCl<sub>2</sub> were purchased from Sigma-Aldrich (St Louis, MO, USA). The phosphate assay kit was purchased

from Amresco (Solon, OH, USA). Penicillin, streptomycin, Dulbecco's modified Eagle's medium (DMEM), Roswell Park Memorial Institute (RPMI) medium 1640, and Dulbecco's phosphate buffered saline (DPBS) were purchased from GIBCO (Grand Island, NY, USA). Fluo-4-AM was purchased from Invitrogen (Burlington, Ontario, Canada). Fetal bovine serum (FBS) was purchased from Hyclone (Logan, UT, USA). Water soluble tetrazolium (WST-1) was purchased from Biovision (Mountain View, CA, USA).

### Preparation of metal-LSB complexes

Na-LSB, K-LSB, Mg-LSB, and Zn-LSB complexes were prepared in 1 mL of H<sub>2</sub>O by mixing LSB (to a final concentration of 10 mmol/L) with NaOH (20 mmol/L), KOH (20 mmol/L), Mg(OH)<sub>2</sub> (10 mmol/L), or Zn(OH)<sub>2</sub> (10 mmol/L), respectively. To prepare Cr-LSB, Mn-LSB, Co-LSB, and Ni-LSB complexes, LSB (10 mmol/L) was first precipitated with NaOH (20 mmol/L) in 1 mL of ethanol, and the precipitate was then dissolved by adding CrCl<sub>3</sub>, MnCl<sub>2</sub>, CoCl<sub>2</sub>, or NiCl<sub>2</sub> (10 mmol/L) to form a metal-LSB complex.

### Inhibition of Na<sup>+</sup>/K<sup>+</sup>-ATPase by metal-LSB complexes

The activity of Na<sup>+</sup>/K<sup>+</sup>-ATPase was determined by measuring the amount of inorganic phosphate (Pi) liberated from ATP<sup>[20]</sup>. A commercial Na<sup>+</sup>/K<sup>+</sup>-ATPase from porcine cerebral cortex (Sigma, 0.3 units/mg) was added to 500 μL of the reaction solution containing 1 mmol/L ATP, 3 mmol/L MgCl<sub>2</sub>, 48 mmol/L NaCl, 12 mmol/L KCl, and 24 mmol/L Tris-HCl (pH 7.8). The enzymatic reaction was terminated by adding 250 μL of 30% (*w/v*) trichloroacetic acid after the incubation period. After centrifugation at 10000×g for 10 min at 4 °C, the supernatant was diluted 12.5-fold with deionized water. Next, 50 μL of color development reagent provided by the phosphate assay kit was added to the solution. After 30 min of incubation at room temperature, the color intensity was measured at 620 nm on a SpectraMax M2 reader (Molecular Devices, USA). Sodium pump activity was expressed as μmol Pi liberated from ATP by 1 mg of Na<sup>+</sup>/K<sup>+</sup>-ATPase in 1 h. The relative activity was calculated as the level of sodium pump activity in the presence of LSB, metal-LSB complexes, and metal ions when normalized to a control of deionized water only (100%).

### Cell cultures

The human adrenergic neuroblastoma cell line SH-SY5Y<sup>[23]</sup> was kindly provided by Dr Tin-yun HO of the Graduate Institute of Chinese Medical Science at China Medical University in Taiwan, China. SH-SY5Y cells grown in RPMI-1640 culture medium supplemented with 10% FBS and 1% *L*-glutamine were maintained at 37 °C in a humidified atmosphere of 95% air/5% CO<sub>2</sub>. Cell passages were performed every other day by trypsinization. For fluorescence imaging, cells were plated in 3-cm cell culture dishes and grown to 80% confluency (approximately 48 h). H9c2 cells (rat cardiomyoblast cell line) were obtained from the Bioresource Collection and Research Center (Hsinchu, Taiwan, China). H9c2 cells grown in DMEM

supplemented with 10% FBS, 1% penicillin/streptomycin, and 1.5 g of sodium bicarbonate were maintained at 37°C in a humidified atmosphere of 95% air/5% CO<sub>2</sub>. Cell passages were performed every other day by trypsinization. For WST-1 staining, cells were plated in a 96-well culture plate at a density of 1×10<sup>4</sup> cells.

### Intracellular Ca<sup>2+</sup> imaging

Fluctuations in the intracellular Ca<sup>2+</sup> levels of SH-SY5Y cells were tracked and visualized with the preloaded fluorescent Ca<sup>2+</sup>-sensitive dye Fluo4-AM<sup>[21, 24]</sup>. Cell-permeable Fluo4-AM was dissolved in DMSO at a concentration of 4 mmol/L. The dye was then further diluted to 4 μmol/L in RPMI-1640 culture medium. The cells were washed once with DPBS, and then RPMI-1640 culture medium supplemented with 4 μmol/L Fluo4-AM was added to the cells for 30 min in a humidified 5% CO<sub>2</sub> incubator at 37°C. After washing in DPBS and RPMI-1640 culture medium, 25 μmol/L of Mg-LSB, Cr-LSB, Mn-LSB, Co-LSB, Ni-LSB, or ouabain was added to the cells. Ca<sup>2+</sup> fluorescence imaging was monitored at multiple intervals over 20 min. Time-lapse images of live cells loaded with Fluo4-AM were collected using IX71 inverted microscopy (Olympus, Tokyo, Japan). Fluctuations in fluorescence intensity of SH-SY5Y cells treated with metal-LSBs and ouabain were analyzed frame by frame with a Time Series Analyzer<sup>[25, 26]</sup>. This plugin was used to analyze time-lapse image stacks. Cells were selected in a region of interest (ROI), and the fluorescence intensity of each time point was measured.

### Cell viability assay

H9c2 cells were treated with ouabain, LSB and metal-LSB complexes at a concentration ranging from 10 nmol/L to 100 μmol/L for 24 h. Next, these cells were subjected to cell viability assay using WST-1. The absorbance was measured at 440 nm on a SpectraMax M2 reader. Control cells underwent the same conditions without the addition of any drugs. Cell viability is expressed as a percentage of the absorbance of treated cells over the absorbance of control cells.

### NMR spectroscopic studies

LSB was dissolved in 1 mL of ethanol to a final concentration of 15 mmol/L and then precipitated by titrating with NaOH (30 mmol/L). The precipitated LSB was re-dissolved by adding CoCl<sub>2</sub> (15 mmol/L) to the ethanol solution. Ethanol was removed in vacuum, and the dried sample was dissolved in D<sub>2</sub>O. The <sup>13</sup>C NMR spectra of LSB and Co-LSB dissolved in D<sub>2</sub>O were obtained using a Varian Unity Inova-600 NMR spectrometer (Blue Lion Biotech, WA, USA).

### Visible spectroscopic studies

LSB was dissolved in 1 mL of methanol to a final concentration of 15 mmol/L. Next, NaOH (30 mmol/L) was added. CoCl<sub>2</sub> was dissolved in methanol to a final concentration of 400 mmol/L. A titration experiment was performed by sequential addition of the CoCl<sub>2</sub> solution to the LSB preparation in a

quartz cuvette. The spectroscopic changes in the solution were monitored. Visible spectra were obtained using a Jasco V500 spectrometer (Jasco Corporation, Tokyo, Japan).

### Statistical analysis

Data are expressed as the mean±standard error of mean (SEM) of 4 replicates. An analysis of variance (One-way ANOVA) was performed using SPSS 12.0 for Windows. Differences were considered statistically significant at *P*<0.05.

## Results

### Potency of metal-LSB complexes for inhibiting Na<sup>+</sup>/K<sup>+</sup>-ATPase

Three relatively abundant metal ions (Na<sup>+</sup>, K<sup>+</sup>, and Mg<sup>2+</sup>) found in the human body and five transition metal ions (Cr<sup>3+</sup>, Mn<sup>2+</sup>, Co<sup>2+</sup>, Ni<sup>2+</sup>, and Zn<sup>2+</sup>) regarded as trace essential elements in human biological functions were used to form soluble complexes with LSB. The potency of these eight metal-LSB complexes (50 μmol/L) for inhibiting Na<sup>+</sup>/K<sup>+</sup>-ATPase activity was determined and compared with that of LSB (Figure 1A). The results showed that the inhibitory potency of LSB was significantly enhanced by forming a complex with any of the five transition metal ions but not with Na<sup>+</sup>, K<sup>+</sup>, or Mg<sup>2+</sup>. To determine whether the enhancement of inhibitory potency for Na<sup>+</sup>/K<sup>+</sup>-ATPase was due to the presence of metal ions, eight metal ions of equivalent concentrations were subjected to the same assay. The results showed only Zn<sup>2+</sup> affected Na<sup>+</sup>/K<sup>+</sup>-ATPase activity (Figure 1B). Therefore, Zn-LSB was excluded in the subsequent studies of metal-LSB complexes.

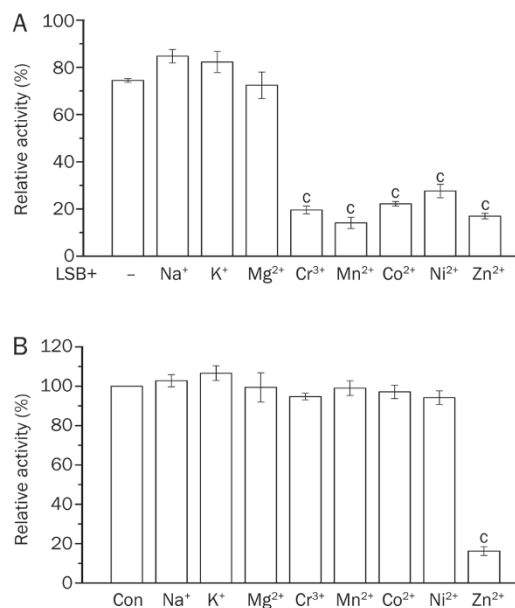


**Figure 1.** (A) The inhibition of porcine Na<sup>+</sup>/K<sup>+</sup>-ATPase by 50 μmol/L of metal-LSB complexes. (B) The inhibition of porcine Na<sup>+</sup>/K<sup>+</sup>-ATPase by 50 μmol/L of the metal ions used in the metal-LSB complexes. The inhibitory potency of the complexes and metal ions was determined by the reduction of Pi liberation from ATP by a constant amount of commercial porcine Na<sup>+</sup>/K<sup>+</sup>-ATPase. The data represent the mean±SEM of five replicates. <sup>c</sup>*P*<0.01 vs LSB only or control group (Con; deionized water only).

Quantitatively, the  $IC_{50}$  value of LSB (101  $\mu\text{mol/L}$ ) and Mg-LSB (128  $\mu\text{mol/L}$ ) was approximately 5 times higher than that of Cr-LSB (23  $\mu\text{mol/L}$ ), Mn-LSB (17  $\mu\text{mol/L}$ ), Co-LSB (26  $\mu\text{mol/L}$ ), or Ni-LSB (25  $\mu\text{mol/L}$ ) (Figure 2).

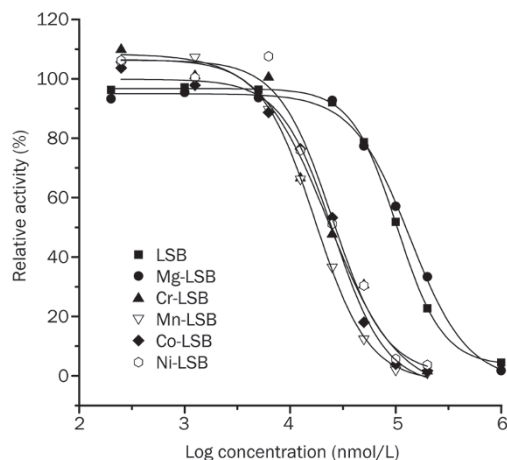


**Figure 2.** The potency of LSB and metal-LSB complexes for inhibiting porcine  $\text{Na}^+/\text{K}^+$ -ATPase. The inhibitory potency of various concentrations of LSB, Mg-LSB and four transition metal-LSB complexes was determined by the reduction of Pi liberation from ATP by a constant amount of commercial porcine  $\text{Na}^+/\text{K}^+$ -ATPase.

#### Effects of metal-LSB complexes on intracellular $\text{Ca}^{2+}$ levels in SH-SY5Y cells

To examine the effects of the four transition metal-LSB complexes ( $\text{Cr}^{3+}$ ,  $\text{Mn}^{2+}$ ,  $\text{Co}^{2+}$ , and  $\text{Ni}^{2+}$ ) on intracellular  $\text{Ca}^{2+}$  levels, SH-SY5Y cells were preloaded with Fluo4-AM and then incubated with 25  $\mu\text{mol/L}$  of a metal-LSB complex or ouabain. Cells were monitored for intracellular fluorescence fluctuations at multiple intervals over 20 min. Compared with cells treated with buffer alone (control), SH-SY5Y cells treated with any of the metal-LSB complexes displayed a significantly elevated fluorescence intensity (Figure 3). These results indicate that the metal-LSB complexes and ouabain increased the intracellular  $\text{Ca}^{2+}$  levels of SH-SY5Y cells.

#### Cytotoxicity of metal-LSB complexes on H9c2 cells

To evaluate the cytotoxicity of the four transition metal-LSB complexes on cardiomyocytes, H9c2 cells were treated with various concentrations (0.01–100  $\mu\text{mol/L}$ ) of these four complexes for 24 h. Next, the cell viability was examined and compared with that of cells treated with the same concentrations of LSB or Mg-LSB (Figure 4). No apparent cytotoxicity was observed in H9c2 cells treated with any of the four transition metal-LSB complexes, except for cells treated with 100  $\mu\text{mol/L}$  of Mn-LSB. Based on these data, H9c2 cells were viable for at least one day when treated with metal-LSB complexes of concentrations lower than 10  $\mu\text{mol/L}$ . Interestingly, the viability of H9c2 cells treated with 100  $\mu\text{mol/L}$  of Co-LSB was substantially higher compared with other treatments. It is possible that Co-LSB increased the

growth or decreased the necrosis of H9c2 cells<sup>[27]</sup>.

#### Identification of the $\text{Co}^{2+}$ -binding site in LSB by NMR spectroscopy

Regarding the paramagnetic properties of the four transition metal-LSB complexes examined, Co-LSB possessed a clear signal pattern in  $^{13}\text{C}$  NMR spectroscopy; therefore, we used this complex to study the interaction between a transition metal and LSB. To identify the  $\text{Co}^{2+}$ -binding site in LSB, the  $^{13}\text{C}$  NMR spectra of LSB and Co-LSB were compared (Figure 5A). In comparison with the  $^{13}\text{C}$  NMR spectrum of LSB, the signals for  $\text{C}8''$ ,  $\text{C}8'''$ ,  $\text{C}9''$ , and  $\text{C}9'''$  were completely eliminated. The signal for  $\text{C}9'$ , but not  $\text{C}9$ , was significantly quenched in the  $^{13}\text{C}$  NMR spectrum of Co-LSB. These data suggest that two carboxylate groups and one carbonyl group of LSB are responsible for coordinating to  $\text{Co}^{2+}$ . The negatively charged carboxylate groups of LSB seem to play a key role in the chelation of the positively charged transition metal ions. Based on our NMR spectral analysis, a 2D structure of Co-LSB is depicted in Figure 5B.

#### Detection of binding modes of LSB and $\text{Co}^{2+}$ by visible spectroscopy

LSB was incorporated with different concentrations of  $\text{Co}^{2+}$ . Next, the d-d orbital electron transition was monitored by visible spectroscopic changes in different binding modes of LSB and  $\text{Co}^{2+}$ . The absorbance of LSB (15 mmol/L) at 400–800 nm was rapidly elevated when the  $[\text{Co}^{2+}]$  increased from 0 to 7.5 mmol/L; however, further elevation of the absorbance was slowed as the  $[\text{Co}^{2+}]$  increased from 7.5 to 15 mmol/L (Figure 6A). No apparent elevation of absorbance was observed when the  $[\text{Co}^{2+}]$  was increased from 15 to 30 mmol/L, except for the absorbance between 500 and 550 nm. This result was observed presumably because of the absorbance of non-coordinated  $\text{Co}^{2+}$ , which has a maximal absorbance at 529 nm in methanol. The titration curve of the absorbance at 420 nm suggested that complexes were formed with a  $\text{Co}^{2+}$ :LSB molar ratio of 1:2 and 1:1 when  $[\text{Co}^{2+}]$  was lower than 7.5 mmol/L and higher than 15 mmol/L, respectively (Figure 6B). The absorbance at 420 nm was minimally elevated and plateaued when the  $[\text{Co}^{2+}]$  was higher than  $[\text{LSB}]$  (15 mmol/L). Obviously, excess  $\text{Co}^{2+}$  could not bind to LSB after forming the Co-LSB complex at a 1:1 molar ratio. The presence of excess  $\text{Co}^{2+}$  existing in its free form is in agreement with the unique elevation of absorbance between 500 and 550 nm when the  $[\text{Co}^{2+}]$  was increased from 15 to 30 mmol/L, as shown in Figure 6A.

#### Discussion

In light of the narrow safety margin and severe side effects of cardiac glycosides in the treatment of congestive heart failure, researchers have extensively searched for potential substitutes isolated from natural sources or novel drugs rationally developed through chemical synthesis and modification<sup>[15, 28–32]</sup>. Side effects are unlikely to be eliminated for candidate drugs that possess the same steroid backbone, or a similar one, as that of cardiac glycosides. In our recent screening of many Chinese medicines used for the promotion of blood

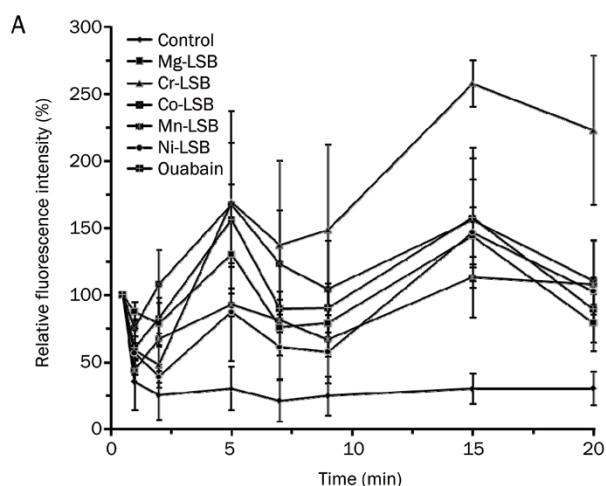
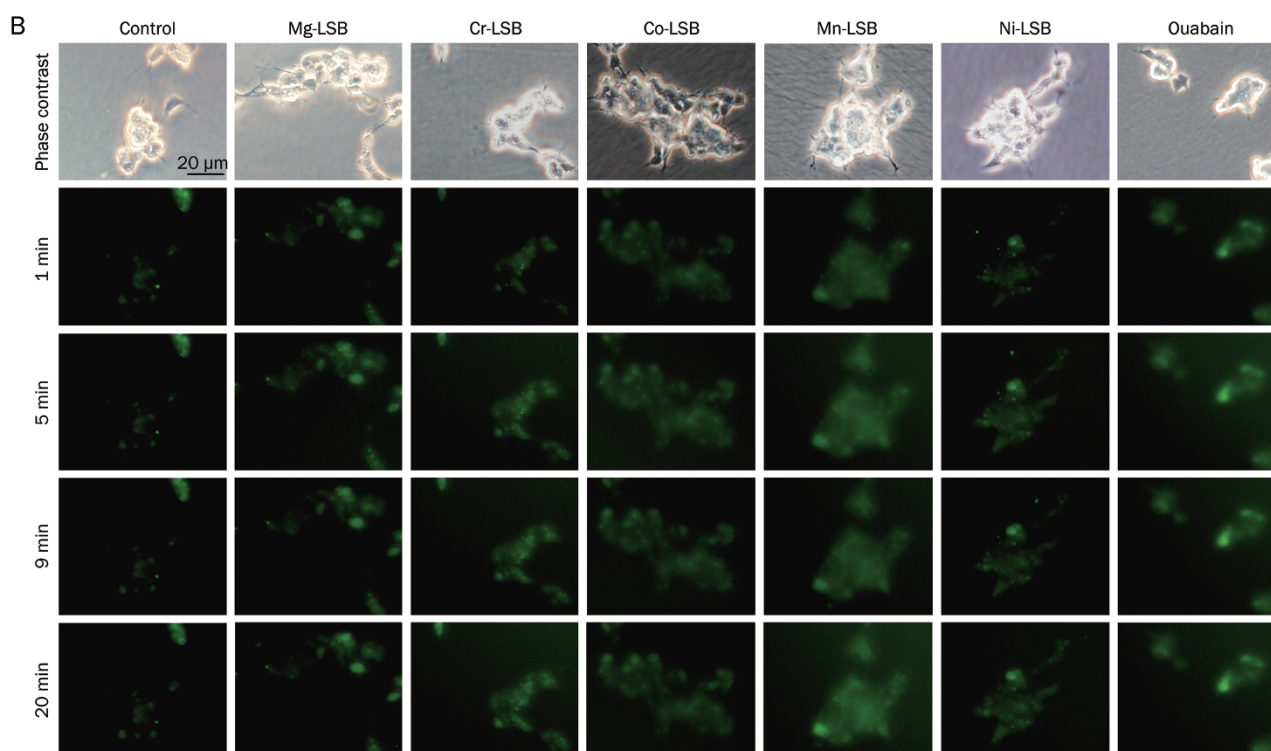


**Figure 3.** Fluctuations in intracellular  $\text{Ca}^{2+}$  levels of SH-SY5Y cells treated with metal-LSB complexes. SH-SY5Y cells were loaded with Fluo4-AM prior to incubation with 25  $\mu\text{mol/L}$  of a metal-LSB complex or ouabain. The intensity of fluorescence was recorded at multiple time intervals over 20 min (A). Each point is representative of time-lapse images in three independent experiments. Serial images of cells treated with metal-LSB complexes and ouabain for 1, 5, 9, and 20 min were captured to display the fluctuation of intracellular  $\text{Ca}^{2+}$  levels (B). The scale bar represents 20  $\mu\text{m}$ .



circulation, numerous analogues of steroid-like compounds were identified as the active ingredient responsible for the therapeutic effect; furthermore, these compounds utilized the same molecular mechanism triggered by cardiac glycosides<sup>[19]</sup>. Surprisingly, Mg-LSB, a non-steroid antioxidant without apparent adverse effects, was identified as the active ingredient in danshen, and it was proposed to be a potential substitute for cardiac glycosides<sup>[20]</sup>. In our current study, we successfully replaced the  $\text{Mg}^{2+}$  of Mg-LSB with transition metal ions. The resulting transition metal-LSB complexes displayed an inhibitory potency approximately 5 times higher than LSB or Mg-LSB. No apparent cytotoxicity from these transition metal-LSB complexes (except for 100  $\mu\text{mol/L}$  Mn-LSB) was observed in cardiomyocytes. Our data suggest

that some of these transition metal-LSB complexes may be superior substitutes for cardiac glycosides in the treatment of congestive heart failure, provided that they undergo necessary clinical trials.

The drastic difference in inhibitory potency for  $\text{Na}^+/\text{K}^+$ -ATPase between Mg-LSB and Co-LSB (Figure 3) indicates that  $\text{Mg}^{2+}$  and  $\text{Co}^{2+}$  might interact with LSB differently. Similar to our observations (data not shown), it has been previously shown that the  $^{13}\text{C}$  NMR spectra of LSB and Mg-LSB are essentially identical<sup>[33]</sup>; more specifically, the signals for  $\text{C}8''$ ,  $\text{C}8'''$ ,  $\text{C}9''$  and  $\text{C}9'''$  of Mg-LSB did not disappear, and the signal for  $\text{C}9'$  of Mg-LSB was not significantly quenched compared with the  $^{13}\text{C}$  NMR spectrum of Co-LSB. Presumably,  $\text{Co}^{2+}$ , but not  $\text{Mg}^{2+}$ , interacts strongly with the two carboxylate groups at

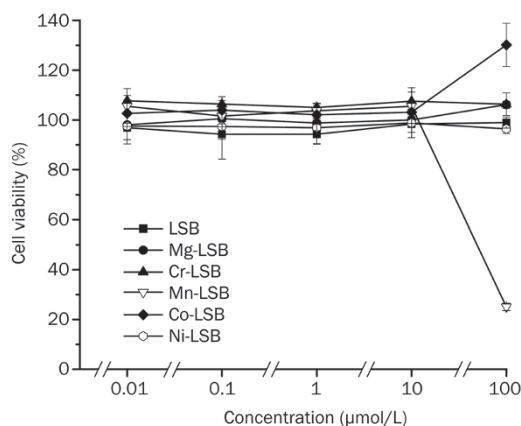


**Figure 4.** The effects of LSB and metal-LSB complexes on the viability of H9c2 cells. H9c2 cells were treated with various concentrations of LSB, Mg-LSB or four transition metal-LSB complexes for 24 h. Cell viability was measured using a WST-1 assay. The data are represented as the mean  $\pm$  SEM ( $n=4$ ; 4 wells in the same experiment).

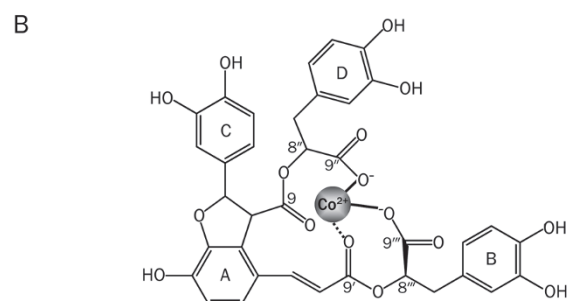
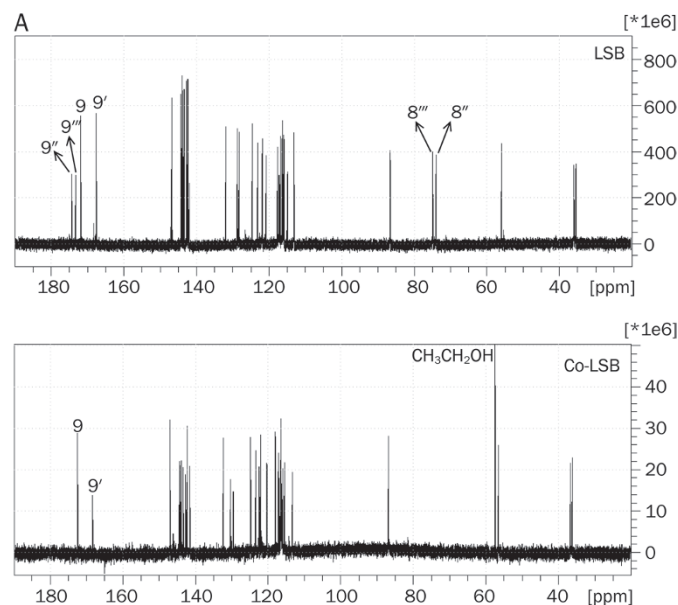


**Figure 5.** (A) The  $^{13}\text{C}$  NMR spectra of LSB and Co-LSB. The NMR signals of C-8'', C-8''', C-9'', and C-9''' in the LSB spectrum indicated by arrows were quenched in the Co-LSB spectrum. The NMR signal of C-9' in the LSB spectrum was substantially reduced in the Co-LSB spectrum when compared with that of C-9. (B) The proposed 2D structure of Co-LSB. The solid and dashed lines between  $\text{Co}^{2+}$  and oxygen atoms of LSB represent strong and weak interactions, respectively.

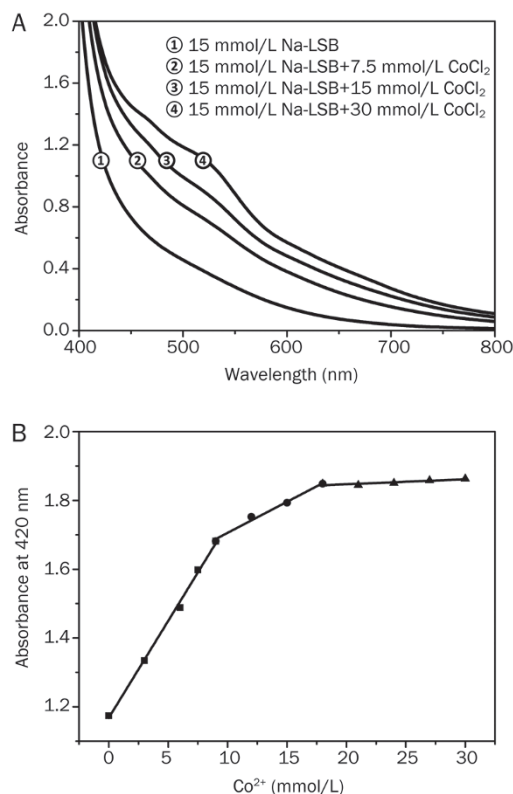


**Figure 6.** (A) The visible spectra of LSB in complex with various concentrations of  $\text{Co}^{2+}$ . (B) The absorbance intensity of LSB titrated against  $\text{Co}^{2+}$  at 420 nm. The change in LSB intensity titrated against  $\text{Co}^{2+}$  could be separated into three parts, including a fast increment from 0 to 7.5 mmol/L, a slow increment from 7.5 to 15 mmol/L, and no obvious change from 15 to 30 mmol/L.

C9'' and C9''' of LSB and weakly with the carbonyl group at C9' of LSB. These interactions likely lead to a more rigid structure of Co-LSB that might be a better fit than Mg-LSB or LSB within the binding pocket of  $\text{Na}^+/\text{K}^+$ -ATPase. The detailed structural differences between Mg-LSB and Co-LSB as well as the variance of their molecular interaction with the residues around the binding pocket of  $\text{Na}^+/\text{K}^+$ -ATPase needs to be investigated.

In terms of chemical characteristics, many active ingredients in Chinese herbs, particularly phenolic compounds clustered with oxygen-containing functional groups, tend to chelate metal ions. Chelation of metal ions might affect the bioactivities of phenolic compounds, such as baicalein and baicalin. These two major bioactive compounds in the Chinese herb *Scutellaria baicalensis* were found to form complexes with  $\text{Fe}^{2+}$  and  $\text{Fe}^{3+}$  that possessed distinctive anti-Fenton properties<sup>[34]</sup>. Similar iron-binding properties of quercetin, the major phenolic compound in cranberries, were also observed and were proposed to be effective at modulating cellular iron homeostasis under physiological conditions<sup>[35]</sup>. Moreover, the biological activities of catechins, the active components in green tea, have been reported to be influenced by metal ions, especially transition metal ions. For example,  $\text{Mn}^{2+}$  was found

to coordinate to the B- and D-rings of epigallocatechin gallate (the most abundant catechin in green tea), while  $Al^{3+}$  tended to coordinate to only the D-ring<sup>[36,37]</sup>. As shown by our findings on enhancing the potency of transition metal-LSB complexes for inhibiting  $Na^+/K^+$ -ATPase activity, we suggest that the chelation of active ingredients from Chinese herbs, by using metal ions, may be an applicable approach to improving the therapeutic effects of these herbs.

### Acknowledgements

The work was supported by a grant to Jason TC TZEN of National Chung-Hsing University, Taiwan, China (NCHU-101D073).

### Author contribution

Jason TC TZEN and Hsin-An CHEN designed the study; Nan-Hei LIN and Tse-yu CHUNG performed the experiments; Feng-yin LI contributed new analytical tools and reagents; and Jason TC TZEN wrote the manuscript.

### References

- Skou JC, Esmann M. The Na,K-ATPase. *J Bioenerg Biomembr* 1992; 24: 249–61.
- Rose AM, Valdes R Jr. Understanding the sodium pump and its relevance to disease. *Clin Chem* 1994; 40: 1674–85.
- Shinoda T, Ogawa H, Cornelius F, Toyoshima C. Crystal structure of the sodium-potassium pump at 2.4 Å resolution. *Nature* 2009; 459: 446–50.
- Morth JP, Pedersen BP, Toustrup-Jensen MS, Sorensen TL, Petersen J, Andersen JP, et al. Crystal structure of the sodium-potassium pump. *Nature* 2007; 450: 1043–9.
- Ogawa H, Shinoda T, Cornelius F, Toyoshima C. Crystal structure of the sodium-potassium pump ( $Na^+,K^+$ -ATPase) with bound potassium and ouabain. *Proc Natl Acad Sci U S A* 2009; 106: 13742–7.
- Lebovitz RM, Takeyasu K, Fambrough DM. Molecular characterization and expression of the ( $Na^+,K^+$ )-ATPase alpha-subunit in *Drosophila melanogaster*. *EMBO J* 1989; 8: 193–202.
- O'Brien WJ, Lingrel JB, Wallick ET. Ouabain binding kinetics of the rat alpha two and alpha three isoforms of the sodium-potassium adenosine triphosphate. *Arch Biochem Biophys* 1994; 310: 32–9.
- Morris JF, Ismail-Beigi F, Butler VP, Gati I, Lichtstein D. Ouabain-sensitive  $Na^+,K^+$ -ATPase activity in toad brain. *Comp Biochem Physiol A Physiol* 1997; 118: 599–606.
- Li-Saw-Hee FL, Lip GY. Digoxin revisited. *QJM* 1998; 91: 259–64.
- Melero CP, Medarde M, San Feliciano A. A short review on cardiotonic steroids and their aminoguanidine analogues. *Molecules* 2000; 5: 51–81.
- Blaustein MP. The interrelationship between sodium and calcium fluxes across cell membranes. *Rev Physiol Biochem Pharmacol* 1974; 70: 33–82.
- Ferrandi M, Barassi P, Molinari I, Torielli L, Tripodi G, Minotti E, et al. Ouabain antagonists as antihypertensive agents. *Curr Pharm Des* 2005; 11: 3301–5.
- Yang Z, Luo H, Wang H, Hou H. Preparative isolation of bufalin and cinobufagin from Chinese traditional medicine ChanSu. *J Chromatogr Sci* 2008; 46: 81–5.
- Chen RJY, Chung TY, Li FY, Lin NH, Tzen JTC. Effect of sugar positions in ginsenosides and their inhibitory potency on  $Na^+/K^+$ -ATPase activity. *Acta Pharmacol Sin* 2009; 30: 61–9.
- Tzen JTC, Chen RJY, Chung TY, Chen YC, Lin NH. Active compounds in Chinese herbs and medicinal animal products for promoting blood circulation via inhibition of  $Na^+,K^+$ -ATPase. *Chang Gung Med J* 2010; 33: 126–36.
- Chen RJY, Chung TY, Li FY, Yang WH, Jinn TR, Tzen JTC. Steroid-like compounds in Chinese medicines promote blood circulation via inhibition of  $Na^+/K^+$ -ATPase. *Acta Pharmacol Sin* 2010; 31: 696–702.
- Chen YC, Liu YL, Li FY, Chang CI, Wang SY, Lee KY, et al. Antcin A, a steroid-like compound from *Anrodiacamphorata*, exerts anti-inflammatory effect via mimicking glucocorticoids. *Acta Pharmacol Sin* 2011; 32: 904–11.
- Chung TY, Li FY, Chang CI, Jinn TR, Tzen JT. Inhibition of  $Na^+/K^+$ -ATPase by antcins, unique steroid-like compounds in *Anrodiacamphorata*. *Am J Chin Med* 2012; 40: 953–65.
- Chen RJ, Jinn TR, Chen YC, Chung TY, Yang WH, Tzen JT. Active ingredients in many Chinese medicines promoting blood circulation are  $Na^+/K^+$ -ATPase inhibitors. *Acta Pharmacol Sin* 2011; 32: 141–51.
- Tzen JTC, Jinn TR, Chen YC, Li FY, Cheng FC, Shi LS, et al. Magnesium lithospermate B possesses inhibitory activity on  $Na^+,K^+$ -ATPase and neuroprotective effects against ischemic stroke. *Acta Pharmacol Sin* 2007; 28: 609–15.
- Chen YC, Jinn TR, Chung TY, Li FY, Fan RJ, Tzen JT. Magnesium lithospermate B extracted from *Salvia miltiorrhiza* elevates intracellular  $Ca^{2+}$  level in SH-SY5Y cells. *Acta Pharmacol Sin* 2010; 31: 923–9.
- Lu Y, Foo LY. Polyphenolics of *Salvia* – a review. *Phytochemistry* 2002; 59: 117–40.
- Biedler JL, Roffler-Tarlov S, Schachner M, Freedman LS. Multiple neurotransmitter synthesis by human neuroblastoma cell lines and clones. *Cancer Res* 1978; 38: 3751–7.
- Aoshima H, Satoh T, Sakai N, Yamada M, Enokido Y, Ikeuchi T, et al. Generation of free radicals during lipid hydroperoxide-triggered apoptosis in PC12h cells. *Biochim Biophys Acta* 1997; 1345: 35–42.
- Balaji J. <http://rsbweb.nih.gov/ij/plugins/time-series.html> 2007.
- Vicencio JM, Ibarra C, Estrada M, Chiong M, Soto D, Parra V, et al. Testosterone induces an intracellular calcium increase by a nongenomic mechanism in cultured rat cardiac myocytes. *Endocrinology* 2006; 147: 1386–95.
- Bi S, Liu JR, Li Y, Wang Q, Liu HK, Yan YG, et al.  $\gamma$ -Tocotrienol modulates the paracrine secretion of VEGF induced by cobalt(II) chloride via ERK signaling pathway in gastric adenocarcinoma SGC-7901 cell line. *Toxicology* 2010; 274: 27–33.
- Kjeldsen K, Norgaard A, Gheorghide M. Myocardial  $Na,K$ -ATPase: the molecular basis for the hemodynamic effect of digoxin therapy in congestive heart failure. *Cardiovasc Res* 2002; 55: 710–3.
- Quadri L, Cerri A, Ferrari P, Folpini E, Mabilia M, Melloni P. Synthesis and structure-activity relationships of 17-(hydrazonomethyl)-5-androstane-3,14-diol derivatives that bind to  $Na^+,K^+$ -ATPase receptor. *J Med Chem* 1996; 39: 3385–93.
- De Munari S, Barassi P, Cerri A, Fedrizzi G, Gobbin M, Mabilia M, et al. New approach to the design of novel inhibitors of  $Na^+,K^+$ -ATPase: 17-substituted seco-D-5-androstane as cassaine analogues. *J Med Chem* 1998; 41: 3033–40.
- Gobbin M, Perez C, Wei Y, Rapoza E, Su G, Bou-Abdallah F, et al. 17-O-aminoalkyloxime derivatives of 3,14-dihydroxy-5-androstane and 3-hydroxy-14-oxo-seco-D-5-androstane as inhibitors of the digitalis receptor on  $Na^+,K^+$ -ATPase. *J Med Chem* 2001; 44: 3821–30.
- Cerri A, Almirante N, Barassi P, Benicchio A, De Munari S, Marazzi G, et al. Synthesis and inotropic activity of 1-(O-aminoalkyloximes) of perhydroindene derivatives as simplified digitalis-like compounds acting on the  $Na^+,K^+$ -ATPase. *J Med Chem* 2002; 45: 189–207.
- Zhang Y, Akao T, Nakamura N, Hattori M, Yang XW, Duan CL, et al.

- Magnesium lithospermate B is excreted rapidly into rat bile mostly as methylated metabolites, which are potent antioxidants. *Drug Metab Dispos* 2004; 32: 752–7.
- 34 Perez CA, Wei Y, Guo M. Iron-binding and anti-Fenton properties of baicalein and baicalin. *J Inorg Biochem* 2009; 103: 326–32.
- 35 Guo M, Perez C, Wei Y, Rapoza E, Su G, Bou-Abdallah F, *et al*. Iron-binding properties of plant phenolics and cranberry's bio-effects. *Dalton Trans* 2007; 41: 4951–61.
- 36 Inoue MB, Inoue M, Fernando Q, Valcic S, Timmermann BN. Potentiometric and  $^1\text{H}$  NMR studies of complexation of  $\text{Al}^{3+}$  with (-)-epigallocatechin gallate, a major active constituent of green tea. *J Inorg Biochem* 2002; 88: 7–13.
- 37 Navarro RE, Santacruz H, Inoue M. Complexation of epigallocatechin gallate (a green tea extract, egcg) with  $\text{Mn}^{2+}$ : nuclear spin relaxation by the paramagnetic ion. *J Inorg Biochem* 2005; 99: 584–8.